



Flight Conflict Detection and Resolution Based on Digital Grid

Yang Yi¹(✉), Ming Tong¹, and LiuXi²

¹ State Key Laboratory of Air Traffic Management System and Technology,
Nanjing 210000, China

nuaa_yang@nuaa.edu.cn

² Nanjing University of Aeronautics and Astronautics, Nanjing 210016, China

Abstract. For high-altitude control area, in order to assist the ground control personnel to monitor short-term flight conflicts in real-time, and to solve the complex flight conflicts that may occur in multi-aircraft from a global perspective, this paper first establishes a spatial digital grid model based on flight safety intervals, and reasonably simplifies the motion model. Secondly, the short-term reachable domain of the aircraft is transformed into grid coordinates, and the numerically dimensioned method is used to obtain the conflicting reachable domain grid coordinates. On the basis of conflict detection, dynamic programming method is used to select the mutually exclusive grid coordinates which are obtained by traversing grid coordinates, and finally the conflict resolution decision of each aircraft is determined by the performance index. The simulation results show that the proposed method can effectively solve the complex flight conflict problem and provide the resolution decision that meets the safety interval and performance constraints before the TCAS (Traffic Collision Avoidance System), while the algorithm time can meet certain real-time requirements.

Keywords: Flight conflict detection and resolution · Grids model · Dynamic programming

1 Introduction

With the rapid development of civil aviation industry, air traffic flow has increased dramatically [1]. In civil aviation alone, in 2018, 610 million passengers were transported, which has an increase of 10.9% over the previous year [2]. Meanwhile, considering that military aviation, airfreight, and other air activities have becoming more frequent, high altitude control areas in China gets more crowded, which leads to higher properties of flight conflict [3].

At present, there are three main ways to prevent flight conflicts: air traffic control deployment (ATC), Airborne Collision Avoidance (TCAS) and visual obstacle avoidance [4, 5]. ATC can command and deploy aircraft from a global perspective, while TCAS can only achieve local conflict resolution. Considering that the present ATC system is a typical man-in-loop decision system [6], in which the control decisions rely on both established control rules and controllers' experience [7]. In order to

detect the flight conflict fast and efficiently and give optimal conflict resolution in complex conditions, many scholars have done relevant research works. In 1964, Reich established the aircraft collision model theory [8], in which the aircraft was assumed to be a cuboid, thus the flight conflict detection only needs to detect whether the point collided with the cuboid. Folton proposed the idea of computational geometry to solve the problem of multi-aircraft collision detection [9], which uses the proximity of Voronoi polygon to reduce the number of detection between two aircraft. Anderson and Lin built a cross-route collision avoidance model based on the conflict area [10]. Erdmann proposed the collision-free path to prevent collisions between aircrafts [11]. The above researches mainly focus on the medium and long-term conflict detection, without considering the maneuverability of multiple aircraft in the short-term detection process. The above methods mainly focus on the medium and long-term conflict detection of aircraft, without considering the maneuverability of multiple aircraft in the short-term detection process.

While this paper focuses on resolving the short-term flight conflict and represents a conflict detection and resolution method based on digital grid partition, which established the spatial grid model to discretize the kinematics model into decision-making model. Through the model transformation, the short-term reachable region of the aircraft can be represented by grid numbers, which can reduce the complexity of the algorithm for multi-aircraft conflict detection. Besides, the dynamic programming algorithm based the grid model is used for solving conflict resolution problems. This method can obtain the conflict resolution in real-time, as a terminal control means, it can reduce the burden of personnel as well as human errors, and provide guarantee for flight safety.

2 Mathematical Model

2.1 Spatial Grid Model

Spatial division is a static division of airspace structure. The standard of flight interval is mainly defined in three directions: vertical interval, longitudinal interval and lateral interval [12], and the safe standard could be the minimum spatial interval or time interval. Referring to RVSM airspace, the safe interval in the vertical direction is 300 m, the safe interval in the longitudinal plane is 20 km. According to the safe interval standard, the airspace can be divided into several grid cells as shown in Fig. 1.

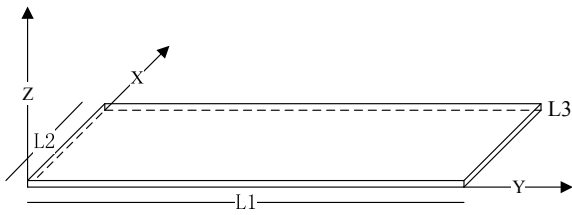


Fig. 1. Grid cell diagram

Figure L_1, L_2, L_3 shows the safety distance in each direction. The entire airspace is divided according to the cell grid shown in the above figure, and the coordinates of each aircraft position can be converted into grid coordinates. Since the length, width and height of the grid are determined by the safety distance, any two aircraft can satisfy the conflict-free flight only by satisfying the following equation.

$$|X_1 - X_2| > 1 \parallel |Y_1 - Y_2| > 1 \parallel |Z_1 - Z_2| > 1 \quad (1)$$

where X, Y, Z , respectively, represent the grid coordinates of the aircraft, and the subscripts represent the aircraft number. It can be seen that maintaining a safe distance between the aircraft only needs to ensure that at least one cell grid is arranged between the aircraft as shown in (1).

Under the conflict-free condition of the airspace model, the minimum grid coordinate difference between the aircraft is 2. The ultimate distance of the real position of the aircraft appears at the boundary of the unit grid, the minimum distance L_1, L_2, L_3 , the maximum distance $3L_1, 3L_2, 3L_3$, and the distance interval is 100–300% of the safety distance. The model guarantees the safety of multi-aircraft flight and the rapidity of conflict detection by sacrificing part of the airspace.

2.2 Aircraft Model

Simplify the model by combining civil aviation flight and ATC characteristics:

1. The speed of the aircraft remains the same.
2. Radar control is applied to the ground [13], assuming that the position and velocity direction information of all aircraft can be obtained.
3. In order to ensure the airworthiness of the aircraft, the available overload can be limited to a certain range.
4. Only for short-term conflicts within the reachable domain of each aircraft.

3 Conflict Detection and Solution Algorithm

3.1 Conflict Detection

Based on the above model, this paper mainly studies short-term conflict detection, that is, conflicts occurring in the next few seconds to several minutes [13]. The existing airborne TCAS system can provide traffic consultation 40 s in advance and provide decision consultation 20 s in advance [14]. However, the TCAS system needs to ensure that the answering machines of both parties do not malfunction and are not interfered by other signals. In the event of an abnormal situation or when TCAS has not yet provided the decision-making consultation stage, the ATC-B can obtain the positional speed information of the aircraft using the broadcast automatic correlation monitoring (ADS-B) to participate in the short-term collision detection and release process of the aircraft [15].

Due to the influence of the wake of the aircraft, considering the safe distance between the aircraft and the flight in the same direction, the detection time of the aircraft is defined as:

$$T = n\Delta t = n \frac{d}{V} \tag{2}$$

where, $n \in N$ represents the predicted step size, and the speed of the aircraft is determined. To ensure the applicability of the algorithm, the maximum prediction time T is not less than the consultation time provided by the TCAS system for 20 s, thereby determining that the maximum of n is $n_{\max} = 6$, and the area that can be reached at each period time is shown in Fig. 2.

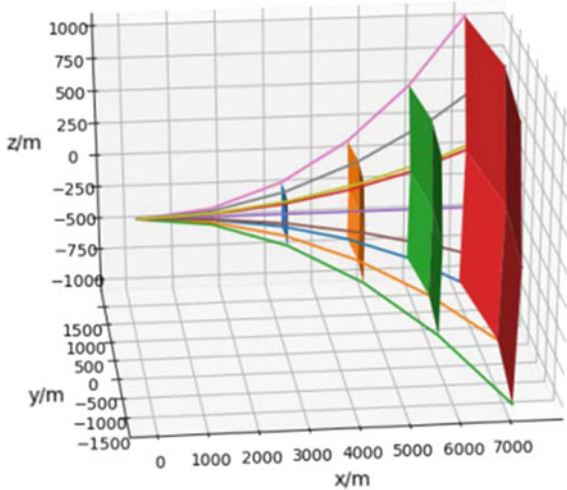


Fig. 2. Aircraft arrival area at different times

For the m-frame aircraft in the high-altitude control area, the traditional conflict detection method is used to compare the positions of every two aircrafts using different strategies at different moments. The comparison times are at least:

$$O_1(m) = n_{\max} A_{\text{num}}^m \tag{3}$$

The amount of computation of the above equation increases significantly with the increase in the number of aircraft. In this paper, the spatial grid model is proposed, and the coordinates of the n_{\max} nodes corresponding to each trajectory are converted into corresponding grid coordinates. The conversion is as follows:

$$\begin{cases} X = \prod(x/L_2) \\ Y = \prod(y/L_1) \\ Z = \prod(z/L_3) \end{cases} \quad (4)$$

X, Y, Z denotes the grid coordinates, numerically annotate the grid coordinate boundary of each node and its internal region, set the initial value $N = 0$ of the non-forbidden flight zone grid, the initial value of the no-fly zone grid $N = 1$, perform the following operations on the values corresponding to the grid coordinates:

$$N = N + 1 \quad (5)$$

According to the above method, the cross-section of the numerical labeling of a single aircraft at the node position is shown in Fig. 3.

0	0	0	0	0	0
0	1	1	1	1	0
0	1	2	2	1	0
0	1	1	1	1	0
0	0	0	0	0	0

Fig. 3. Single aircraft collision-free numerical labeling cross-section

When multiple aircraft collide, the numerical labeling cross-sections at the conflict position are shown in Fig. 4.

1	1	1
2	3	2
2	2	2
1	1	1

(a) Aircraft 1

1	1	1
2	2	2
2	3	2
1	1	1

(b) Aircraft 2

Fig. 4. Multi-aircraft conflict numerical labeling cross-section

The node grid coordinates of (a) and (b) are located at adjacent positions, and after summing with each other, the value is an outlier with a numerical value greater than 2. If the coordinate corresponding to the value is not the node grid coordinate, it may be composed of the boundary 1 of multiple aircrafts, which has no practical significance.

The outliers shown in the above figure correspond to the node grid coordinates, so the two aircraft cannot simultaneously adopt the maneuvering mode to reach the coordinates.

Similarly, for the flight conflict caused by the airspace limitation, the no-fly zone grid is processed by the numerical labeling method in the initialization process, and the form is the same as above, as shown in Fig. 3.

The basic flow chart for short-term collision detection of aircraft is as shown in Fig. 5.

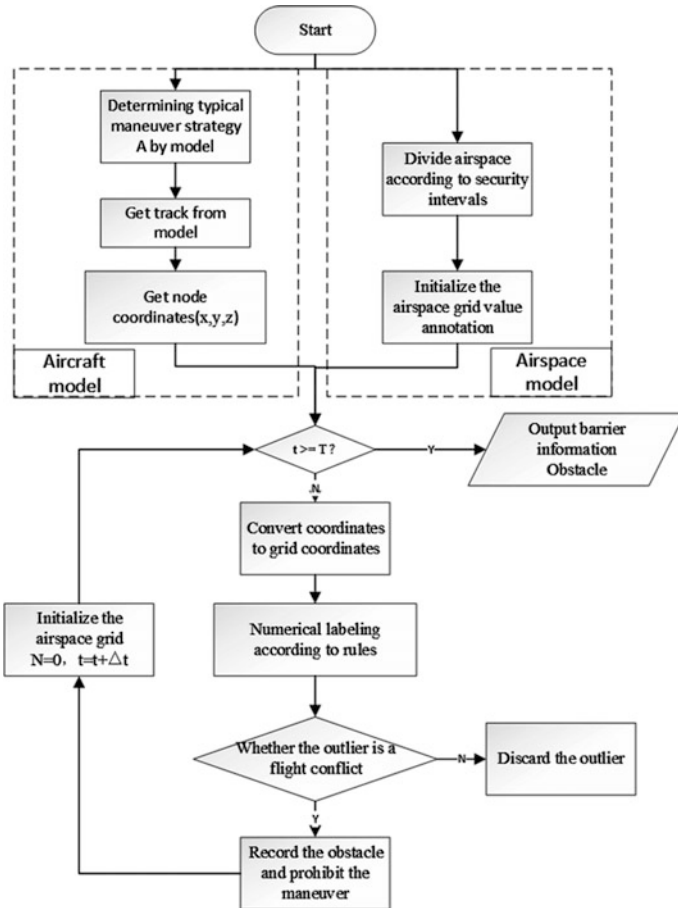


Fig. 5. Flow chart of aircraft conflict detection

Referring to the above process, according to the aircraft model, maneuver strategy and environment model, the predicted position set at each time can be obtained. Considering the flight conflict detection of m aircraft, the detection complexity can be calculated as follows:

$$O_2(m) = 2 \sum_{n=0}^{n_{\max}} mP(n\Delta t) \quad (6)$$

where, the complexity is mainly caused by P . The reference (11) is related to the choice of maximum time and maneuvering strategy, which mainly affects the reachable region boundary. Coefficient 2 detects the outliers after assignment, its complexity increases linearly with the number of aircraft, which is much less than the exponential growth of (3), and the complexity of summation calculation is much less than that of calculating relative distance.

Traditional conflict detection aims at mid-and long-term flight conflicts and only relieves them based on rule base, which can't guarantee the effectiveness of relief in the case of large number of aircraft. This paper mainly focuses on the conflict in the reachable area of short-term aircraft. The method of digital grid can not only greatly reduce the detection complexity of the conflict in the reachable area of short-term aircraft, but also provide a reliable basis and guarantee for conflict resolution.

3.2 Conflict Resolution

In this paper, conflict resolution is based on the aforementioned conflict detection methods. The conflict information *Obstacle* obtained in the detection process mainly includes the node grid coordinates X_e, Y_e, Z_e where the conflict occurs and the corresponding maneuvering strategies of each aircraft. However, for the complex conflict situation of multi-aircraft, firstly, we need to analyze the relationship between the grid coordinates of the collision nodes. Reference (1) compares the grid coordinates of each node, determines the grid coordinates of the collision nodes and classifies them into the same collision. At the same time, we can get the number of the aircraft and the maneuvering mode. When satisfying the constraints of dynamics and velocity dip angle, the conflict resolution is transformed into the selection process of strategy, that is, According to the above conflict information, the maneuvering decision of each aircraft is reasonably selected by planning method to maximize the total performance index. The flow chart for distinguishing collision node grids is shown in Fig. 6.

In the figure above, *Connect* is a multivariate combination leading to conflict, the elements in which is corresponded to the discriminant between the aircraft number F as well as the decision number O of arriving at the conflict location, which can be obtained by (1). By traversing to conflicting combinations (F_1O_1, F_2O_2) , the maneuvering strategies in the combinations will not conflict in different moments. Therefore, there is at least one of the decisions a is negated in all combinations (F_1O_1, F_2O_2) , and all decisions a can be combined into action sets *action* as follows:

$$\text{action}(t) = \left\{ (a, \dots) \mid a = (FO_1, \dots, FO_i), FO_i \in (FO_{i1}, FO_{i2}), (FO_{i1}, FO_{i2}) \in \text{Connect}(t) \right\} \quad (7)$$

After obtaining the action set without conflict, the initial state of the aircraft can be set to execute all the decisions included in the decision.

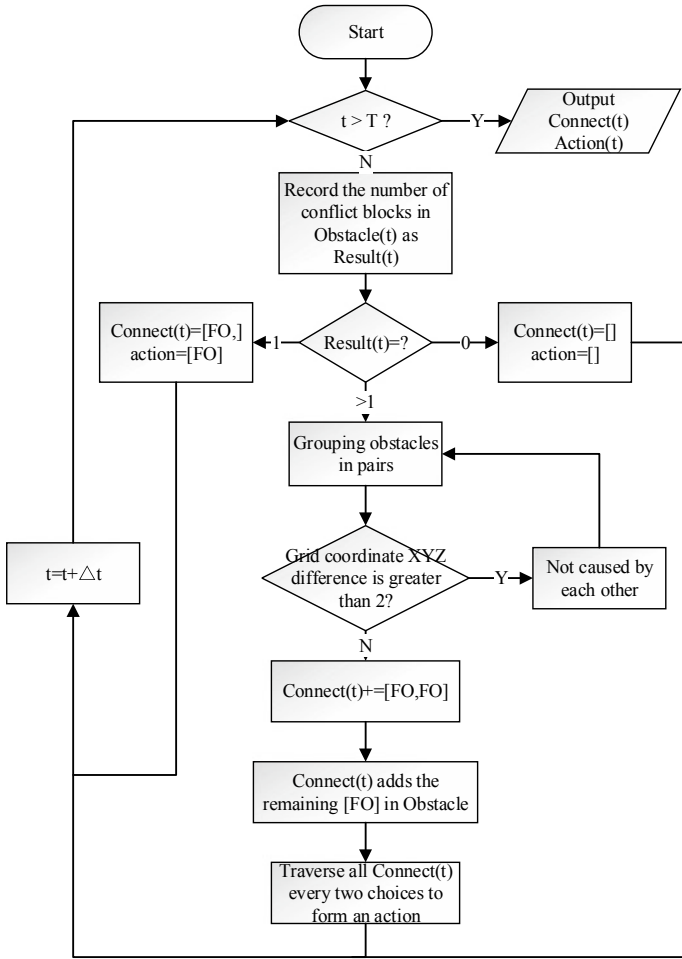


Fig. 6. Flight conflict matching and action output

$$S = \{(s_1, \dots, s_m) | s_i = (A_0, \dots, A_{num})\} \tag{8}$$

The initial state will change under *action*. s_i represents the executable strategy set of aircraft i . Considering the performance constraints of aircraft, the executable strategy of aircraft is further restricted. That is, when the velocity inclination angle is too large (too small), the strategy of upward (downward) maneuver should not be adopted. The executable strategy S of all aircraft satisfies no aftereffect, that is, the future is only related to the current state, but not to the past state. The state transition process can be expressed as follows:

$$S_t \xrightarrow{\text{action}(t)} \prod \theta S_{t+\Delta t} \tag{9}$$

where $\prod\theta$ represents the constraint of satisfaction, S_t represents the set of policies that can be adopted at the current time, and $S_{t+\Delta t}$ represents the set of policies that can be adopted at the next prediction time. In the process of state transition, $\text{action}(t)$ functions as follows:

$$S_{t+\Delta t} = \prod_{\theta} (S_t - S_a) \tag{10}$$

where,

$$S_a = FO, FO \in a \tag{11}$$

where, FO represents the maneuvering strategy corresponding to the O -th decision-making number of the F -th aircraft, that is, the maneuvering mode that the aircraft cannot adopt.

According to the state transition process (10), the state of each aircraft at the next prediction time is updated continuously, and finally S_T is obtained by iteration. At this time, the executable strategy set of any two aircraft has met the safety requirement (1). Design optimization performance indicators as following:

$$J = \text{opt}_{a \in \text{action}} \sum_{i=0}^m \min K_i(s_i)M, \quad s_i \in S_T \tag{12}$$

where, S_T represents the set of executable strategies of the aircraft at the maximum predictive time, which is determined by the state transition in (16), and K in (20) represents the performance indicators of each aircraft under the current executable strategy, which is specifically expressed as:

$$K = \sqrt{(x_t - x_{\text{end}})^2 + (y_t - y_{\text{end}})^2 + (z_t - z_{\text{end}})^2} \tag{13}$$

The end subscript represents the position coordinates of the target point of the aircraft, and t is determined by the following equation:

$$t = \text{step} * \Delta t \tag{14}$$

where, Δt is the predicted time interval and step is the updated step in the simulation process, which affects the release decision-making and simulation operation efficiency of the aircraft. Equations (12), (13), and (14) give the final release decision for each aircraft:

$$(F_0 \dots F_m) = \arg \min_{(A_0 \dots A_m)} \left(\arg \min_S J \right) \tag{15}$$

By seeking the smallest performance index J to obtain optimal parameters S and combining (13), the nearest decision (A_0, \dots, A_m) from the target point can be obtained. F represents aircraft in (15). Each aircraft updates its position, velocity, and direction by the decision, and finally reaches the target point.

The complexity of the algorithm above is mainly embodied in the use of obstacle information to form a mutually exclusive combination of aircraft and obstacle numbers, and the final feasible strategy is obtained according to these combination iterations. Multiple traversal combinations can greatly reduce the dimension of combinations and the number of iterations. Further, dynamic programming performance indicators are only related to the final state and a large number of unreasonable states can be eliminated in the iteration process.

4 Simulation Verification

A typical flight conflict is designed and simulated in this paper to validate the effectiveness of the proposed flight conflict detection and resolution algorithm based on digital grid.

The spatial grid and coordinate system are shown in Fig. 1, in which the size is determined by the safe interval distance with $L_1 = L_2 = 5000$ m, $L_3 = 300$ m. The executable strategy of an aircraft is shown in Fig. 2. In order to ensure that the maximum predicted distance is larger than the final RA range of TCAS, the maximum predicted step size $n_{\max} = 6$ is set. The starting and ending points of five aircraft satisfy the following formats:

$$\begin{aligned}
 fl &= [V, [x, y, z], [x_{\text{end}}, y_{\text{end}}, z_{\text{end}}], \theta, \psi] \\
 fl_0 &= [280, [5, 5, 8], [95, 95, 8], 0, \pi/4] \\
 fl_1 &= [280, [5, 95, 8], [95, 5, 8], 0, -\pi/4] \\
 fl_2 &= [280, [95, 5, 8], [5, 95, 8], 0, 3\pi/4] \\
 fl_3 &= [280, [45, 95, 9], [5, 25, 9], 0, -3\pi/4] \\
 fl_4 &= [280, [55, 5, 7], [95, 75, 7], 0, \pi/4]
 \end{aligned} \tag{16}$$

in which, the position coordinates are in KM units. According to the calculation, the first collide can be obtained after 22.5 s in simulation time (the 20th simulation cycle in the flight step). While the grid coordinates $[3, 10, 30, -20]$ are set as the no-fly zone, and the aircraft 3 encounters the no-fly zone. The aircraft 4 is added to verify the rapidity of the algorithm for multi-aircraft. The flight trajectory of the collision detection and resolution algorithm presented in this paper is shown in Fig. 7.

It can be seen that two different methods can ensure the safety interval between aircraft, aircraft and no-fly zone. Different maneuvering methods have different maneuvering modes and the same performance index. Because of the setting of safe distance and maneuverability, all obstacle avoidance is from altitude, and the XY plane can't meet the safety requirements. Vehicle 3 avoids the no-fly zone effectively and finally reaches the target point. The mesh spacing difference and maximum of vehicle 012 are studied separately as shown in Fig. 8.

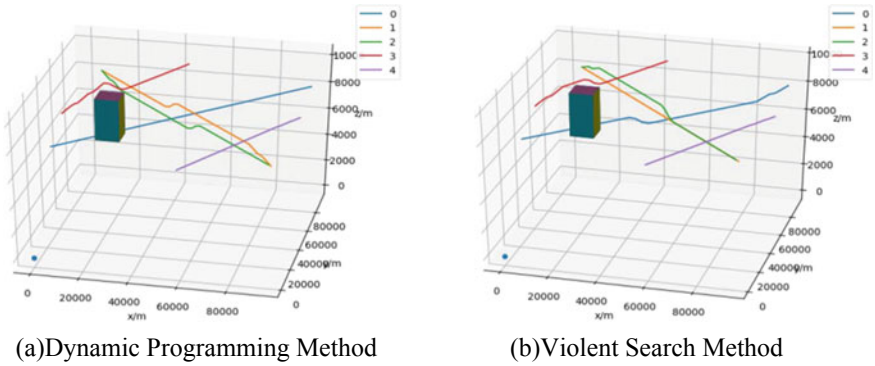


Fig. 7. The flight trajectory diagram of 5 aircraft

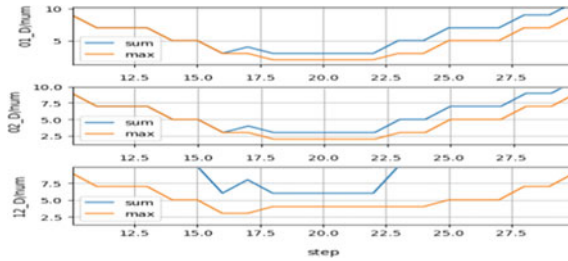


Fig. 8. Aircraft mesh distance map

The graph mainly shows the maximum mesh distance of 012 aircraft during the whole simulation process. From the initial parameter setting, it is known that collision will occur in the 20th simulation cycle. It can be seen from the figure that the safety Formula (1) is satisfied by any two aircraft in the 20th step of collision prediction, i.e., the flight safety interval requirement. The distance of their real trajectory is shown in Fig. 9.

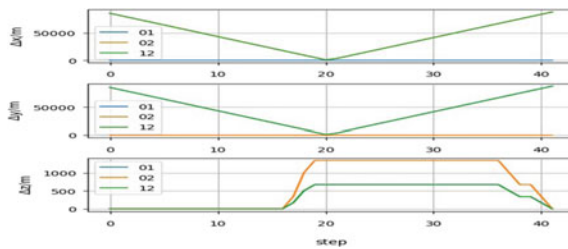


Fig. 9. Distance map of aircraft

To ensure real-time conflict detection and resolution, the whole flight conflict detection and resolution time of the two methods is as shown in Fig. 10.

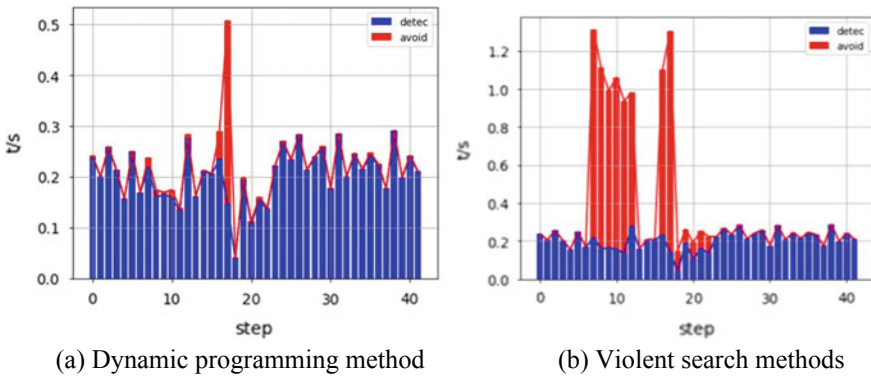


Fig. 10. Detection release time

Flight conflicts are detected by aircraft in the 7th and 18th cycles. The detection time is shorter than 0.3 s on Python platform. In post-conflict detection, the violent search method takes longer time to extricate, which does not meet the real-time requirements, while the dynamic programming method takes shorter time. It can ensure a certain real-time performance on other computing platforms for the dynamic programming method.

5 Conclusions

In order to ensure air traffic safety and reduce the situation of controllers in the complex conflict conditions of multiple aircraft, this paper proposes a method based on digital grid to detect and release flight conflicts. This method improves the automation performance of the air traffic control system. The main advantages are: (1) The prediction range is larger than the recommended decision range of the aircraft TCAS system, auxiliary air traffic controllers make command decisions on multiple aircraft; (2) Provides conflict resolution optimal solutions for TCAS system failures or unreliable conditions. The conflict detection and liberation in this paper are based on the digital grid model of the airspace which sacrifices part of the space and greatly simplifies the calculation of the safety interval. The motion model of the aircraft is fully considered to obtain the reachable area for collision detection, and the dynamic planning method is used to obtain all the non-conflicting maneuver state combinations of each aircraft. Finally, the optimal conflict resolution decision is obtained according to the performance index. At the same time, the current liberation algorithm still has some shortcomings, and the related problems of the simulation algorithm data structure and optimal parameters need to be further optimized.

References

1. He SUN, Yueru CAI, Wei ZHOU (2016) Prediction of aircraft multi-machine flight conflict status. *Comput Simul* 33(6):59
2. Qifeng Q (2010) Research on anti-collision strategy in air traffic management. Southwest Jiaotong University, Chengdu
3. Minggong W, Zekun W, Xiangxi W (2019) Geometric optimization model for flight conflict relief. *Syst Eng Electr*
4. Chen Z (2016) Technical challenges faced by future air traffic control system development. *Command Inf Syst & Technol* 7(6):1–5
5. Yan Y, Cao G (2018) Operational concepts and key technologies of next generation air traffic management system. *Command Inf Syst & Technol* 9(3):8–17
6. Reich PG (1966) Analysis of long-range air traffic system: separation standards. *J Ins Navig* 19(1, 2, 3)
7. Aurenhammer F (1991) Voronoi diagrams—a survey of fundamental geometric data structure. *ACM Comput Surveys* 23(3):9
8. Anderson D, Lin XG (1996) Collision risk model for a crossing track separation methodology. *J Navig* 49(2):337–349
9. Mao ZH, Feron E, Bilmoria K (2000) Stability of intersecting aircraft flows under decentralized conflict avoidance rules. In: AIAA guidance navigation and control conference, Denver, CO, pp 14–17
10. Air Traffic Control Committee of the Central Military Commission of the State Council (2002) Flight Interval Standard 5, 31
11. ICAO (1998) Handbook on airspace planning methods for determining interval standards. ICAO document, Doc. 9689-AN/953
12. Bicchi A, Marigo A, Pappas G, Pardini M, Parlangei G, Tomlin C, Sastry S (1998) Decentralized air traffic management systems: performance and fault tolerance. In: Proceedings IFAC workshop on motion control
13. Li P (2013) Research on the detection and release strategy of flight conflicts. China Civil Aviation Flight Academy
14. Zhang A (2018) Research on simulation technology of TCASII collision avoidance model. China Civil Aviation College
15. Luo WT, Zhao ZR, Zhang DY (2011) Investigation of aircraft collision avoidance and early warning algorithm based on ADS-B. *Control Eng China* 4:559–563